

# Nanophase Separation in Monodisperse Rodcoil Diblock Polymers

L. H. Radzilowski and S. I. Stupp\*

Department of Materials Science and Engineering, Department of Chemistry, Materials Research Laboratory and Beckman Institute for Advanced Science and Technology, University of Illinois at Urbana-Champaign, Urbana, Illinois 61801

Received April 11, 1994; Revised Manuscript Received August 31, 1994\*

**ABSTRACT:** We have observed nanophase-separated structures in rodcoil polymers synthesized in our laboratory. Each polymer consists of a perfectly monodisperse, rodlike segment covalently bonded to a coil-like segment of polyisoprene such that both rod and coil share the same molecular backbone. The polyisoprene was prepared by living anionic polymerization, and thus the rodcoil diblock molecules in the systems studied are of fairly uniform molar mass. Annealing of solution-cast thin films approximately 5–10 nm thick leads to ordered nanoscale morphologies that depend upon the volume fraction of rod segments in these diblock molecules. We find by transmission electron microscopy that the morphology varies from alternating strips of rod- and coil-rich domains to discrete aggregates of rods arranged in a hexagonal superlattice as rod volume fraction is decreased. At an intermediate volume fraction we see a coexistence of strips and aggregates. This breakup of rod domains may be the result of entropic coil stretching penalties analogous to those postulated recently by Williams and Fredrickson in lamellar assemblies of rodcoils.

## Introduction

A hallmark of block copolymer behavior is the interdependence of enthalpic interactions and conformational entropy on microphase-separated morphology as the relative volume fraction of blocks varies. Block copolymers that consist of a molecularly rigid block coupled to a flexible block may affect profoundly this thermodynamic interdependence and lead to unique microphase-separated states. In a recent communication<sup>1</sup> we reported on the synthesis of a monodisperse "rodcoil" diblock polymer containing one rigid and one flexible segment joined covalently to share the same molecular backbone and showed it to phase separate into alternating rod- and coil-rich domains with in-plane dimensions of less than 10 nm. This experimental system has enabled us to study further their "nanophase" separation behavior, particularly in light of recent theoretical predictions and the lack of previous experimental work using monodisperse systems. We use the term "nanophase" to emphasize that our system forms structures with dimensions which are not common in microphase-separated flexible copolymers. The high immiscibility between rod and coil segments for enthalpic and entropic reasons allows block segregation to occur at relatively smaller values of  $N$  than in typical flexible copolymers.

An interesting aspect of rodcoil polymers is of course the abrupt change in backbone rigidity at the rodcoil junction. Theoretical work has shown that conformational asymmetry can alter the shape of phase diagrams as well as shift the boundaries between ordered phases to different volume fractions.<sup>2</sup> Theoretical work by Schweizer has further shown that stiffness asymmetry must be weighted together with intermolecular interactions of the different chemical species when predicting phase behavior.<sup>3</sup> Bates et al. have experimentally found shifts in ordered phase boundaries<sup>4</sup> and an increase in the Flory  $\chi$  parameter with increasing stiffness asym-

metry.<sup>5</sup> Rodcoil polymers viewed in this context would be an extreme case, and order-disorder transitions could be expected at relatively high temperatures or low degrees of polymerization. Theoretical work by Semenov and Vasilenko<sup>6</sup> and Halperin<sup>7</sup> has dealt more explicitly with the relation between rodcoil polymer phase behavior and molecular aggregation. Flexible segments of coil-coil block copolymers pack in a liquidlike fashion even though coil conformations are deformed from a Gaussian state in the strong segregation limit. By contrast the rigid and prolate shape of rod segments might preclude an amorphous or even radial arrangement due to sterics and thus space-filling difficulties. Such rod structures would lack uniform density unless flexible coils are allowed to penetrate. A layered, or smectic, arrangement of rods with their long axes aligned would solve the problem, especially at large values of the Flory  $\chi$  parameter. But smectic ordering of rods would also confine the rod-coil junctions to a flat interface with a relatively high density of grafting sites, giving the coils little additional volume to explore away from the interface. Analogous to a planar brush, this additional confinement would exacerbate coil stretching and make a greater entropic contribution to the free energy balance. To help relieve stretching, rods within a layered structure may undergo a tilting transition<sup>7,8</sup> or transform from bilayers to monolayers,<sup>6</sup> while Raphaël and de Gennes<sup>9</sup> and Williams and Fredrickson<sup>10</sup> predict that molecular layers may break into discrete micellar structures allowing more volume for coils to explore. At the same time smectic rodcoil phases may have additional enthalpic energy contributions due to rods at the edges of the layered phases making unfavorable contact with coils. The addition of these unique entropic and enthalpic factors will likely be manifest in the morphology and properties of rodcoil polymers, especially as parameters such as rod volume fraction and  $\chi$  are varied.

Only a limited number of experimental studies have been performed on rodcoil copolymer systems. Three previous studies involved systems in which side chain liquid crystal polymers were coupled to flexible blocks.<sup>11–13</sup> In one of these studies microphase separa-

\* To whom correspondence should be addressed at the Department of Materials Science and Engineering.

† Abstract published in *Advance ACS Abstracts*, November 1, 1994.

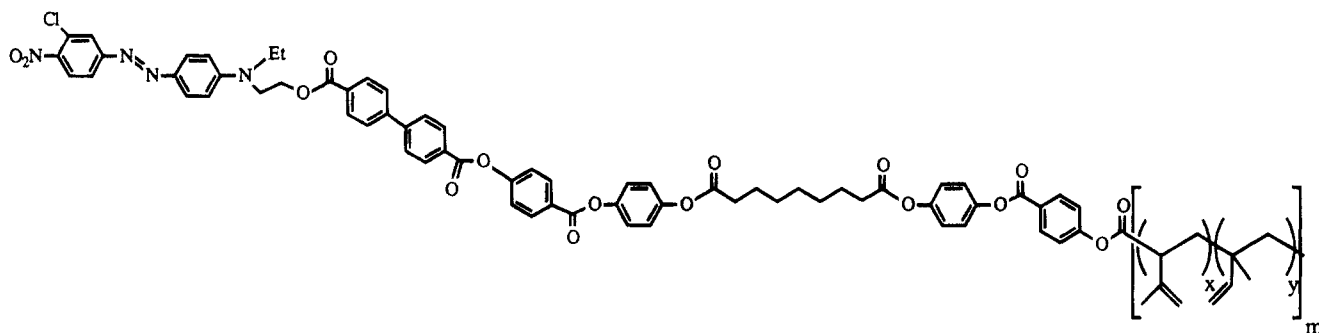


**Figure 1.** Chemical structure of the rodcoil polymers studied here. The structural units of the polyisoprene segments result from 3,4 addition (*x*) (~71%) and 1,2 addition (*y*) (~29%).

tion into lamellae was reported based on transmission electron microscopy (TEM) of microtomed sections,<sup>11</sup> while in another study spheres of polystyrene in a continuous liquid crystalline matrix were observed by TEM.<sup>13</sup> Work has also been performed on systems consisting of conducting polymer blocks coupled to flexible ones to form linear diblocks. For example, Cohen et al.<sup>14</sup> observed lamellar, cylindrical, and spherical microphase-separated domains in diblocks of polyacetylene and polynorbornene, although they did not comment on molecular packing of the rigid blocks. In a similar vein systems consisting of polypeptide blocks in  $\alpha$ -helical conformation as the rigid segment coupled to flexible blocks such as polybutadiene or non- $\alpha$ -helical polypeptides have been synthesized. Lamellar mesophases were observed in solution by small-angle X-ray scattering (SAXS), with the polypeptide block being either folded<sup>15</sup> or extended and tilted.<sup>16</sup> TEM of solution-cast films has revealed cylindrical<sup>17</sup> and lamellar<sup>18</sup> microdomains, with the degree of microphase separation and microdomain dimensions depending on the type of solvent used. While coil blocks in these "main chain" rodcoils were reported to have relatively low polydispersities (1.05–1.10), the polypeptide rod blocks had broader distributions of molar mass. Polypeptides of low polydispersity are difficult to synthesize by nonbiological methodologies, and most of the previous work required fractionation of rod blocks to narrow the distribution. Polydispersity, however, causes adverse effects on block copolymer behavior, such as broadening the distribution of domain sizes and the range of temperatures at which the order–disorder transition (ODT) occurs.<sup>19</sup> The effects have been predicted to become significant at polydispersities on the order of 1.3 and higher.<sup>20</sup> Polypeptides additionally are prone to folding, complicating the interpretation of microstructural observations.<sup>15,16</sup> Well-defined systems should facilitate experimental observations and the testing of current theories.

In this paper we examine the morphology of our rodcoil diblock polymer by TEM as a function of varying rod volume fraction and consider our results within the framework of theoretical predictions by Williams and Fredrickson.<sup>10</sup> Their work recognizes the additional constraints of rodcoil systems and attempts to predict the morphology of domains by calculating free energies of the possible phases.

## Experimental Section

**Materials.** The rodcoil polymer studied here has the chemical structure shown in Figure 1 and was synthesized using the procedure described in an earlier publication.<sup>1</sup> The synthesis and chemical characterization of these materials were first described in a previous publication, and additional

**Table 1.** Coil Molecular Weight Data

coil $\bar{M}_n$	polydispersity index	rod volume fraction, $f_{rod}^a$
3200	1.08	0.36
4200	1.04	0.30
5400	1.05	0.25
7600	1.05	0.19

<sup>a</sup>  $f_{rod}$  is calculated as  $R^2L/(R^2L + r^2Nb)$ , where  $R$  = the hard core radius of the rod,  $L$  = the extended length of the rod,  $r$  = the hard core radius of a polyisoprene segment,  $N$  = the degree of coil polymerization, and  $b$  = the length of an isoprene repeat unit (after Semenov and Vasilenko<sup>6</sup>).

details are described elsewhere.<sup>21</sup> For this work a series of polyisoprene segments with varying molecular weights were synthesized and coupled to the rod segment to create the range of volume fractions listed in Table 1. The polymers studied contained polyisoprene segments in which 71% of the structural units formed by 3,4 addition and 29% by 1,2 addition. The rod volume fraction ( $f_{rod}$ ) was calculated as  $R^2L/(R^2L + r^2Nb)$ , where  $R$  = the hard core radius of a rod,  $L$  = the extended length of a rod,  $r$  = the hard core radius of a polyisoprene segment,  $N$  = the degree of coil polymerization, and  $b$  = the length of an isoprene repeat unit (after Semenov and Vasilenko<sup>6</sup>). As indicated in Table 1, the polymers studied had low polydispersities.

**Transmission Electron Microscopy.** Characterization of rodcoil morphology was performed on a Philips CM-12 at 100 kV. Specimens were prepared by first dissolving the rodcoil polymer in cyclohexane (0.05 wt %), a good solvent for the coil but poor for the rod, followed by rapid stirring for several hours. Droplets of the dilute solution were placed onto carbon-coated glass slides in a solvent atmosphere. The solvent evaporated after approximately 30 min, and films were then held under vacuum for at least 24 h. Pieces of the carbon and polymer film were next floated onto water and picked up with copper grids. Samples were examined before and after annealing, which was performed under a constant flow of nitrogen. Annealing temperatures and times ranged from 100 to 150 °C and from 6 to 120 h. Prior to imaging by TEM, specimens were exposed to vapors of an aqueous solution of osmium tetroxide (4%) for 12 h. OsO<sub>4</sub> preferentially stains the unsaturated bonds of the polyisoprene coils, creating amplitude contrast between rod and coil regions. In all of the micrographs shown here, coil domains appear dark and rod ones light.

**Image Enhancement.** The signal-to-noise ratio of TEM images was enhanced by translational Fourier filtering. This technique effectively removes the coefficients of the Fourier transform of a TEM image at those spatial frequencies that do not correspond to the periodic structure of a specimen.<sup>22</sup> Images were first digitized in a Leafscan 35 negative scanner with a spot size of 50  $\mu$ m, giving a sampling size of less than one-fourth of the smallest structural detail observed in the micrograph. Fast Fourier transforms of the digitized images were then taken with software packages such as Image or Suprim. Coefficients of the transform corresponding to structural detail were filtered from those corresponding to noise by multiplying the power spectrum by a "mask" having a value of unity near the coefficients of interest and zero elsewhere.

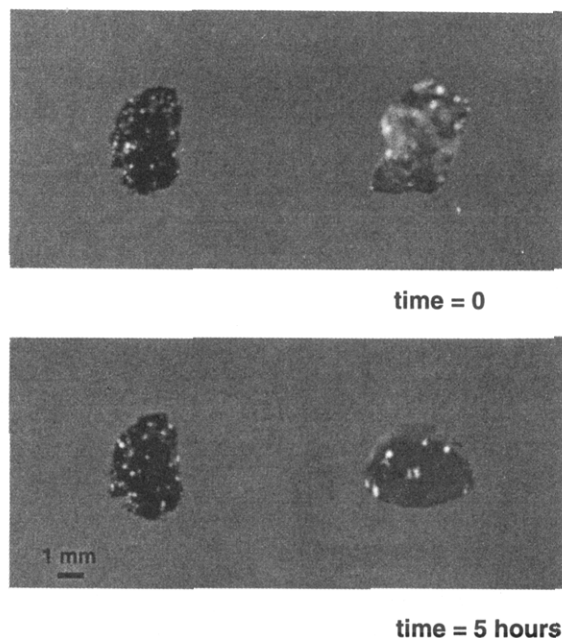


**Figure 2.** Photographs taken 5 h apart of samples of a rodcoil polymer and its corresponding polyisoprene. The homopolymer (at right) flows and changes shape with liquidlike behavior over a period of 5 h whereas the rodcoil polymer retains its shape during this period of time.

Using a mask generated from the parameters of the reciprocal lattice for a particular power spectrum is referred to as lattice-pass filtering. In some cases it was more convenient to apply a mask that retains a larger region of the transform by removing only those coefficients at frequencies higher than a specified threshold, also known as low-pass filtering. Inverse Fourier transforms were then taken to give the filtered images.

## Results and Discussion

The rodcoil polymers studied are red, ductile materials which soften and flow upon heating above room temperature. The softening point increases with the molecular weight of the polyisoprene segment. The rodcoil polymers also have increased stiffness compared to homopolymer polyisoprenes of the same molecular weight. As shown in Figure 2, over a period of 5 h the rodcoil polymer sample retains its shape while a sample of the corresponding polyisoprene flows.

Three of the four rodcoil polymers listed in Table 1 show nanophase separation in the as-cast state with morphology depending on rod volume fraction,  $f_{\text{rod}}$ . Polymers with  $f_{\text{rod}}$  values of 0.36 and 0.30 show rod-rich domains in the shape of narrow strips approximately 7 nm in width and up to 1  $\mu\text{m}$  in length and small, irregularly shaped aggregates 7–10 nm in diameter. The strips can be arranged in parallel or remain isolated in a polyisoprene matrix with the aggregates dispersed in between. This observation was reported in our previous communication.<sup>1</sup> The rodcoil polymer with  $f_{\text{rod}} = 0.25$  displays only the small aggregates of approximately the same size but with weaker contrast between rod and coil domains and less clearly defined domain boundaries. The rodcoil polymer with  $f_{\text{rod}} = 0.19$  does not show nanophase separation in the as-cast state.

Upon annealing, the morphologies transform to periodic structures of rod and coil domains with a shape and size of rod domains that depend on  $f_{\text{rod}}$ . The highest rod volume fraction studied (0.36) transforms to a morphology consisting entirely of alternating rod- and coil-rich strips with more uniform in-plane dimensions

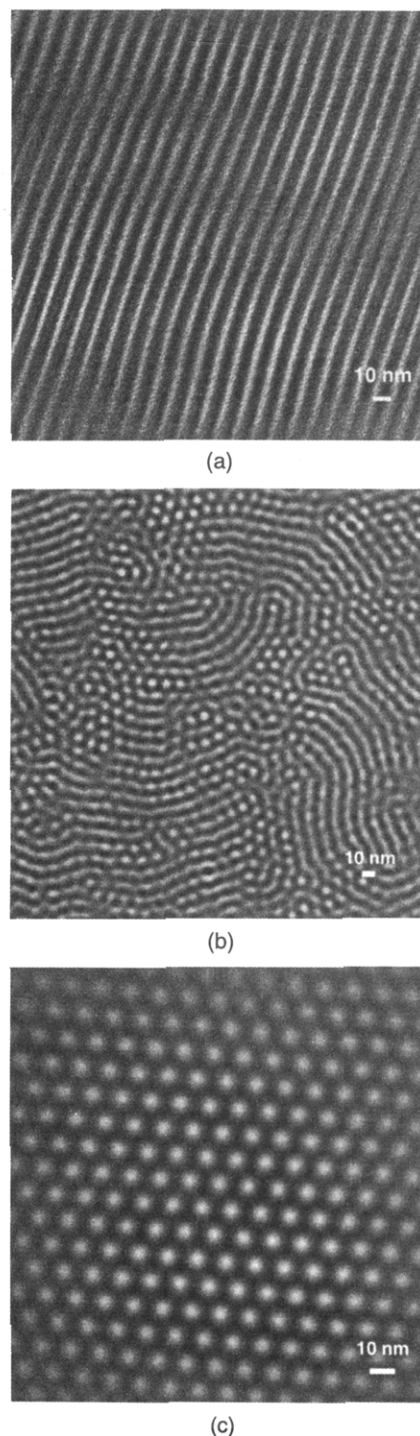


**Figure 3.** Filtered TEM micrographs revealing nanophase separation in three rodcoil polymers studied after annealing at 140 °C for 12 h. (a) Rodcoil polymer with  $f_{\text{rod}} = 0.36$  revealing alternating rod- and coil-rich strips 6–7 and 5–6 nm wide, respectively. (b) A mixed morphology of strips and smaller aggregates is shown in a material of  $f_{\text{rod}} = 0.30$ ; both rod and coil strips measure 6–7 nm wide. (c) Morphology of a sample with  $f_{\text{rod}} = 0.25$ , revealing a hexagonal superlattice of rod aggregates that are approximately 7 nm in diameter spaced 15 nm apart.

than the as-cast as shown in the lattice-pass filtered image of Figure 3a. The rod and coil strips measure 6–7 and 5–6 nm, respectively. An unfiltered image at lower magnification (Figure 4) shows that the direction of the strips' long axis varies in orientation across the film plane in patterns analogous to those of liquid crystalline textures. A low-pass filtered image in the inset of Figure 4 shows the presence of "dislocations"

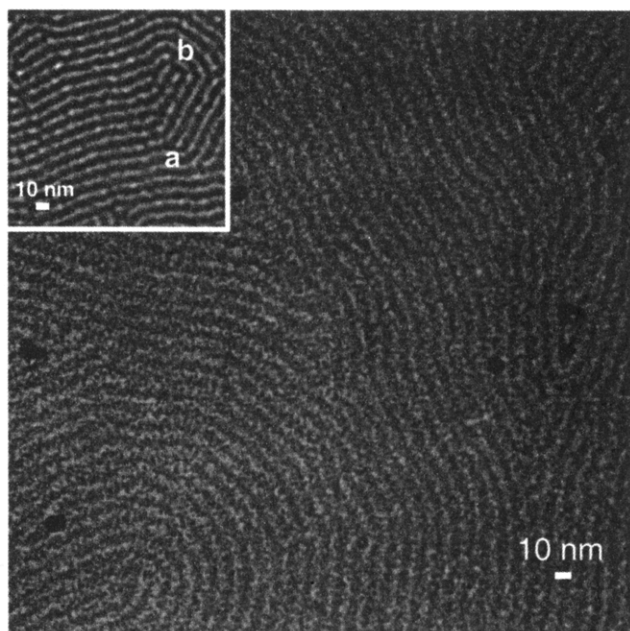


**Figure 4.** Morphology of the rodcoil polymer with  $f_{\text{rod}} = 0.35$  after annealing at 140 °C for 12 h (unfiltered). The inset shows a low-pass filtered image of a smaller area and reveals a "dislocation" (a) and a disclination of the type  $s = +1/2$  (b).

and a disclination of the type  $s = +1/2$ . The polymers with the two smallest volume fractions organize into morphologies of discrete and uniformly sized rod domains dispersed in a matrix of polyisoprene coils. As shown in the lattice-pass filtered image in Figure 3c, the aggregate-like domains of the sample with  $f_{\text{rod}} = 0.25$  organize into a superlattice with hexagonal order, measure approximately 7 nm in diameter, and have an average interdomain spacing of 15 nm. The shape of the aggregates should not be inferred from the filtered image as being smooth and round. The filtering process, while removing high-frequency noise, also removes fine detail from the real structure. An unfiltered image of aggregates is shown in Figure 5. The left inset is the power spectrum of a smaller area indicating hexagonal symmetry. Finally, at a rod volume fraction of 0.30 the morphology appears to have characteristics of both strip and aggregate volume fractions. When annealed at 140 °C the morphology consists of both strip and aggregate domains (Figure 3b). The fraction of strips vs aggregates varies randomly over the sample plane, and rod- and coil-rich strips as well as aggregates measure 6–7 nm in width. As indicated by the arrow in Figure 6 the aggregates form rows that in places extend along the same direction as strips. This morphology resembles cylinders of coil-coil block copolymers that are oriented both parallel and perpendicular to the sample plane. However, tilting the rodcoil thin film samples about a single axis in the film plane reveals that both strip and aggregate rod domains have approximately equal thickness in the direction perpendicular to the film plane (Figure 7). The domain thickness is also approximately equal to the domain width in the film plane. *Therefore these TEM images cannot be interpreted as corresponding to cylinders of different orientation.* Finally, this coexistence may not be the equilibrium structure at this volume fraction; however, annealing for longer time periods and higher temperatures does not lead to a significant change.

The increase in order of rodcoil domains upon annealing likely reflects an approach toward thermodynamic equilibrium from the as-cast state. Annealing

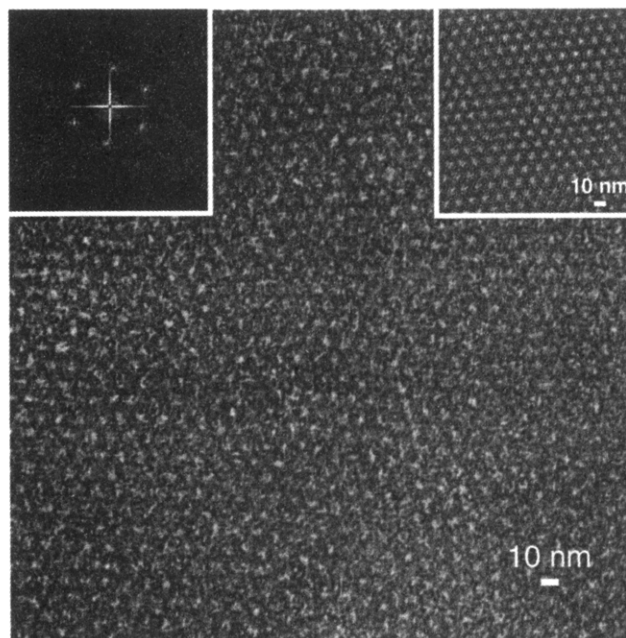


**Figure 5.** Unfiltered image of the rodcoil polymer with  $f_{\text{rod}} = 0.25$  annealed at 140 °C for 12 h. The power spectrum of a smaller area in the left inset reveals hexagonal ordering of aggregates. The right inset shows a smaller area that has been Fourier lattice-pass filtered using the first three orders of the corresponding hexagonal reciprocal lattice.

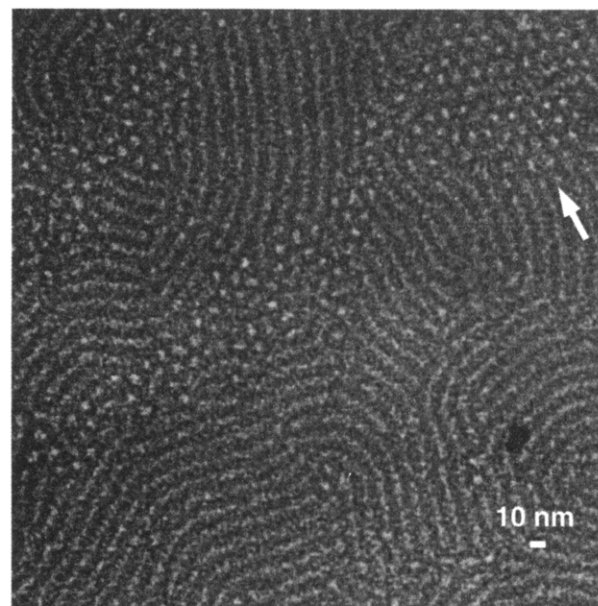


**Figure 6.** Unfiltered TEM image of rodcoil polymer having  $f_{\text{rod}} = 0.30$ . The arrow points to an example of how the aggregates form rows in alignment with strips. Both rod and coil strips are 6–7 nm wide.

at temperatures below 130 °C for any duration has little apparent effect while annealing above 140 °C causes a reduction or loss in long-range order. The fact that ordered morphologies are observed after quenching suggests that during annealing samples are not in a disordered state. The crystal to liquid crystal transition of the neat rod segment is 140 °C, suggesting that in the 130–140 °C range molecules have the mobility needed to improve domain ordering. We do not know if annealing above 140 °C results in an order-disorder transition or chemical changes such as cross-linking of the polyisoprene coils. Above this temperature the system may alternatively undergo a transition from the nanophase-separated state into a nematic state. Inter-



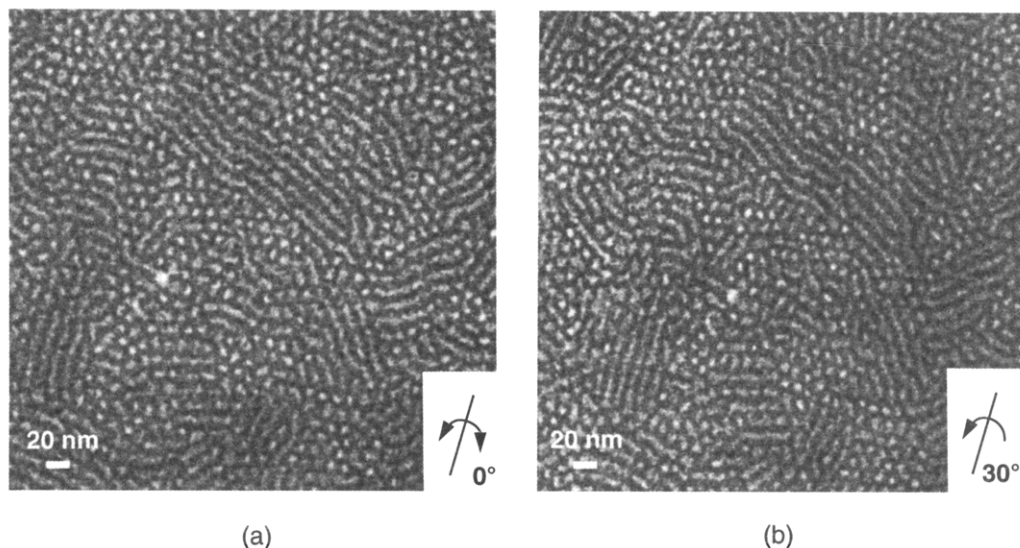


**Figure 7.** TEM micrographs from the same region of a film of rodcoil polymer having  $f_{\text{rod}} = 0.30$ . (a) Projected image taken at a tilt angle of  $0^\circ$  to the specimen normal. (b) Projected image taken at a tilt angle of  $30^\circ$  to the specimen normal.

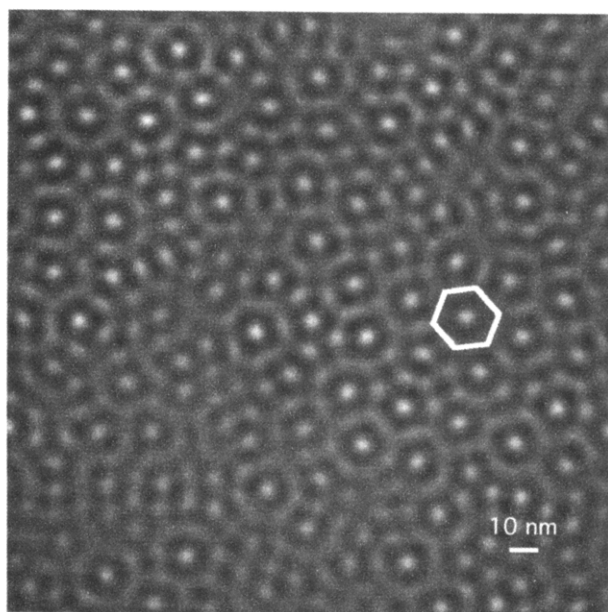


**Figure 8.** A thick section of a rodcoil sample with  $f_{\text{rod}} = 0.30$  revealing a network of hexagonally shaped cells, each containing a rod aggregate in the center.

estingly, annealing the  $f_{\text{rod}} = 0.19$  material at  $140^\circ\text{C}$  appears to disrupt definition and order among aggregates. Annealing near  $100^\circ\text{C}$ , on the other hand, produces a hexagonal superlattice with long-range order comparable to  $f_{\text{rod}} = 0.25$  (Figure 3c). In coil-coil block copolymers  $T_{\text{ODT}}$  occurs at higher values of  $\chi N$  as chains become increasingly asymmetric in volume fraction, requiring either lower temperatures or larger  $N$  to maintain an ordered state. The behavior of rodcoil polymer with  $f_{\text{rod}} = 0.19$  could be similarly interpreted as not having a large enough  $N$  to remain in an ordered state when annealed at  $140^\circ\text{C}$ .

In thicker regions of rodcoil polymer film we observe morphology different from that on the thinnest regions. For example, the  $f_{\text{rod}} = 0.30$  sample produced a structure consisting of rod domains that appear to form the sides of cell-like structures with apparent hexagonal symmetry, each one containing a single aggregate in the center as shown in Figure 8. Upon annealing, thick rodcoil films consist of terraced, stacked layers. The morphologies shown in Figure 3 are found in single

layers, which have a thickness in the range of 5–10 nm based on the tilting experiment described in Figure 7. Morphologies such as that shown in Figure 8 result from the superposition of layers with some degree of registration between them. The structures of these films will be discussed in detail in a subsequent publication.

The observation of rod domains having smaller lateral dimensions with decreasing rod volume fraction may be a consequence of entropic coil stretching penalties. This observation is reminiscent of coil-coil block copolymer behavior where a change in the volume fraction of the constituent blocks requires a change in the relative amount of interfacial surface area and coil stretching in order to maintain a uniform density, producing the familiar lamellae, cylinders, and spheres. As discussed earlier, based on analogies to polymer brushes rodcoils may experience enhanced coil stretching due to the high “grafting density” at the rod-coil interface. In a recent paper Williams and Fredrickson<sup>10</sup> postulate that lamellae of rodcoils will break apart into discrete fragments or cylindrical micelles in order to relieve coil stretching. A model of their “hockey puck” cylindrical micelle is illustrated in Figure 9. These micelles allow more volume for the coils to explore away from the interface and thus reduce chain stretching.

The conditions under which the puck entity gains a free energy advantage over lamellae is an issue addressed by the calculations of Williams and Fredrickson. In their model of a puck (Figure 9) the coils emanate from a flat surface in such a way as to fill a hemispherical volume on both sides of a puck. The coils are assumed to be strongly stretched as they move away from the surface with straight trajectories. The angle between their trajectory and the surface normal is constant for a given location of the grafting site and increases with distance from the puck center. Beyond the hemisphere the coils are less strongly stretched as they can adopt trajectories radial to the puck center and are free to explore an increasing volume. The stretching free energy is thus calculated using contributions from both inside and outside the hemisphere and as a function of the grafting position. Coils near the puck center will have more repeat units in a highly stretched conformation than those grafted near the edge. The stretching free energy is given by

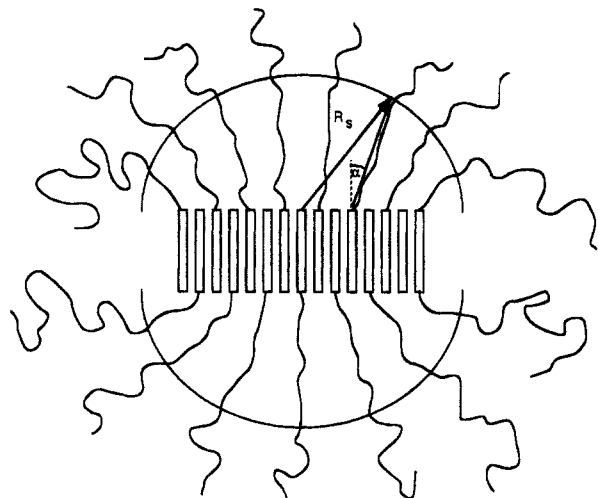


**Figure 9.** Schematic representation of the cross section of an aggregate of rodcoil molecules. In the calculations by Williams and Fredrickson the hemisphere that encloses coils emanating from the puck surface has a radius  $R_s$ . Each coil follows a straight line trajectory through the hemisphere, making an angle  $\alpha$  with the surface normal. For coils grafted further from the center,  $\alpha$  will progressively increase, and after the coil passes through the hemisphere it follows a radial trajectory. Experimentally, the nature of rod packing (layered versus nematic) remains unknown.

$$F_s = \frac{\pi\sigma^2 v R_p^3}{2a^2} \left[ f(\varrho) + \frac{1}{4\varrho} - \frac{1}{4} \left( \frac{2R_p/L}{3\sigma d^2 \lambda} \right)^{1/3} \right] \quad (1)$$

where  $\varrho$  is the ratio of the hemisphere radius,  $R_s$ , to the puck radius,  $R_p$ ,  $\sigma$  is the grafting density,  $d$  is the rod diameter,  $L$  is the rod length,  $a$  is proportional to the root-mean-square distance between neighboring Gaussian repeat units of volume  $v$ , and  $\lambda$  is the ratio of coil to rod volume fractions. The first term,  $f(\varrho)$ , describes the chain stretching energy for all coils emanating from a puck surface up to the hemisphere. It is calculated considering how the volume per coil repeat changes with distances from the puck surface to the hemisphere surface. Smaller changes in this volume reflect greater degrees of coil stretching. The second term is the contribution from those parts of the coils that have passed through the hemisphere. Thus, there is a  $\varrho$  value that optimizes the portion of coils outside the hemisphere.

Analysis of the minimized free energy shows two regimes of scaling behavior. When the puck radius,  $R_p$ , is sufficiently small, the coils can fill and pass through the hemisphere. If, however, the puck radius is large such that the coils cannot completely fill up the hemisphere, then they will essentially form a planar brush. In this case the stretching free energy of coils is not reduced since they remain confined and thus cannot explore the increasing amount of volume available outside the hemisphere. The stretching free energy of the moplike puck is found to scale as  $R_p^3$  and the brushlike puck as  $R_p^2$ . This difference reflects the physical behavior of coils. As the degree of stretching of a brush is essentially uniform throughout its height, the brushlike puck will have a stretching free energy proportional to the amount of puck area. But since the coils of the moplike puck can explore a hemispherical shell after passing a distance roughly the height of the brush, chain stretching has greater sensitivity to  $R_p$ . Whether a moplike puck or a lamellar phase is favored will therefore depend on the free energy balance between coil stretching and the lateral surface energy due

to exposed edges of rod domains. The complete free energy is given by

$$F_\gamma + F_{ms} - F_{ls} \propto \frac{2^{1/2}(\nu\chi_s)^{1/2}}{x} + \frac{\lambda x}{4\kappa} \left( \beta - \frac{1}{4} \left( \frac{4x}{3\lambda} \right)^{1/3} \right) - \frac{\lambda^2}{16\kappa} \quad (2)$$

where the first term is the lateral surface free energy, the second term is the coil stretching free energy in monolayer pucks, the third term measures coil stretching in monolayer lamellae,  $\kappa = Na^2/L^2$ ,  $\nu = \kappa/\lambda$ , and  $x = R_p/L$ . As this equation shows, the free energy of the lamellar phase increases with the square of the coil volume fraction, driving the above free energy difference more negative and hence stabilizing the puck phase.

While the predictions of Williams and Fredrickson do not consider how micellar structures will order with respect to each other in bulk nor thin films, they are nonetheless useful for our initial understanding of the morphology of rodcoil thin films. A pair of tilted images similar to Figure 7 for the largest  $f_{rod}$  studied (0.36) shows that the thickness of rod domains in the direction perpendicular to the film plane is comparable to their width in the film plane. Similarly the aggregate domains of  $f_{rod} = 0.25$  have approximately equal thickness and width. The in-plane size of rod domains clearly decreases as  $f_{rod}$  decreases. In the context of calculations by Williams and Fredrickson one may understand this as the breakup of strips to produce smaller aggregates (see Figure 3c) in which less confinement and stretching of coils occurs, thus lowering their total free energy. The observation of both types of structure at  $f_{rod} = 0.30$  points to the concept of a breakup driven by chain stretching penalties as we see rows of aggregates in register with strips.

A question of interest is how rodcoil morphologies compare with those of coil-coil block copolymers. The rod domains termed strips are analogous to cylinders of coil-coil block copolymers. The possible modes of rod packing discussed earlier suggest these domains are monolayers or bilayers of rods forming boards or strips rather than cylinders. With regard to aggregate domains, their dimensions appear too small to be radially arranged extended rod segments. We do not yet know the details of rod packing within domains to conclude if these are the "pucks" described by Williams and Fredrickson. The value of  $f_{rod} = 0.36$  (strips) correspond to the region between lamellae and the OBDD structure in coil-coil diblock copolymers. At the value  $f_{rod} = 0.25$  where aggregates form, cylinders are observed in flexible copolymers. This lack of correspondence is not surprising given the extreme stiffness asymmetry.

## Conclusions

Rodcoil polymers were observed to organize into nanophase-separated morphologies that differ significantly as a function of rod volume fraction. The rod segments organize into domains of smaller in-plane dimensions in response to an increase in the coil's degree of polymerization. These domains can take the form of long strips or smaller aggregates of uniform size that organize into superlattices. The striplike rodcoil assemblies break up into smaller domains possibly to reduce coil stretching.

**Acknowledgment.** This work was supported by National Science Foundation Grant DMR 89-20538, obtained through the Materials Research Laboratory of

the University of Illinois. The electron microscopy work was carried out in the Center for Microanalysis of Materials, University of Illinois, which is supported by the U.S. Department of Energy under Contract DEFG02-91-ER45439. Image enhancement was performed in the Beckman Institute Visualization Laboratory with the assistance of Bridget O. Carragher. John L. Wu of our laboratory synthesized the rodcoil polymers, and L.H.R. gratefully acknowledges Eastman Kodak for a graduate fellowship.

## References and Notes

- (1) Radzilowski, L. H.; Wu, J. L.; Stupp, S. I. *Macromolecules* **1993**, *26*, 879.
- (2) Vavasour, J. D.; Whitmore, M. D. *Macromolecules* **1993**, *26*, 7070.
- (3) Schweizer, K. S. *Macromolecules* **1993**, *26*, 6050.
- (4) Rosedale, H. J.; Schulz, M. F.; Koppi, K. A.; Hamley, I. W.; Bates, F. S. APS March Meeting, Seattle, 1993.
- (5) Bates, F. S.; Schulz, M. F.; Rosedale, J. H. *Macromolecules* **1992**, *25*, 5547.
- (6) Semenov, A. N.; Vasilenko, S. V. *Sov. Phys.-JETP (Engl. Transl.)* **1986**, *63*, 70.
- (7) Halperin, A. *Macromolecules* **1990**, *23*, 2724.
- (8) Semenov, A. N. *Mol. Cryst. Liq. Cryst.* **1991**, *209*, 191.
- (9) Raphaël, E.; de Gennes, P.-G. *Makromol. Chem., Macromol. Symp.* **1992**, *62*, 1.
- (10) Williams, D. R. M.; Fredrickson, G. H. *Macromolecules* **1992**, *25*, 3561.
- (11) Adams, J.; Gronski, W. *Makromol. Chem., Rapid Commun.* **1989**, *10*, 553.
- (12) Kodaira, T.; Mori, K. *Makromol. Chem.* **1992**, *193*, 1331.
- (13) Bohnert, R.; Finkelmann, H. *Macromol. Chem. Phys.* **1994**, *195*, 689.
- (14) Saunders, R. S.; Cohen, R. E.; Schrock, R. R. *Macromolecules* **1991**, *24*, 5599.
- (15) Perly, B.; Douy, A.; Gallot, B. *Makromol. Chem.* **1976**, *177*, 2569.
- (16) Douy, A.; Gallot, B. *Polymer* **1987**, *28*, 147.
- (17) Nakajima, A.; Hayashi, T.; Kugo, K.; Shinoda, K. *Macromolecules* **1979**, *12*, 840.
- (18) Barenberg, S.; Anderson, J. M.; Geil, P. H. *Int. J. Biol. Macromol.* **1981**, *3*, 382.
- (19) Henderson, C. P.; Williams, M. C. *J. Polym. Sci., Polym. Phys. Ed.* **1985**, *23*, 1001.
- (20) Spontak, R. J.; Williams, M. J. *J. Polym. Sci., Polym. Phys. Ed.* **1990**, *28*, 1379.
- (21) Wu, J. L. Ph.D. Dissertation, University of Illinois, 1993.
- (22) Misell, D. L. In *Practical Methods in Electron Microscopy*; Glauret, A. M., Ed.; North-Holland: New York, 1978; Vol. 7.